

## Self-organized titanium oxide nanodot arrays by electrochemical anodization

Po-Lin Chen, Cheng-Tzu Kuo, Tzeng-Guang Tsai, Bo-Wei Wu, Chiung-Chih Hsu, and Fu-Ming Pan

Citation: *Applied Physics Letters* **82**, 2796 (2003); doi: 10.1063/1.1571661

View online: <http://dx.doi.org/10.1063/1.1571661>

View Table of Contents: <http://scitation.aip.org/content/aip/journal/apl/82/17?ver=pdfcov>

Published by the [AIP Publishing](#)

---

### Articles you may be interested in

[Nanoscale lateral switchable rectifiers fabricated by local anodic oxidation](#)

*J. Appl. Phys.* **110**, 024511 (2011); 10.1063/1.3609065

[Tunable self-organization of nanocomposite multilayers](#)

*Appl. Phys. Lett.* **96**, 073103 (2010); 10.1063/1.3318262

[Titanium nanostructural surface processing for improved biocompatibility](#)

*Appl. Phys. Lett.* **89**, 173902 (2006); 10.1063/1.2361279

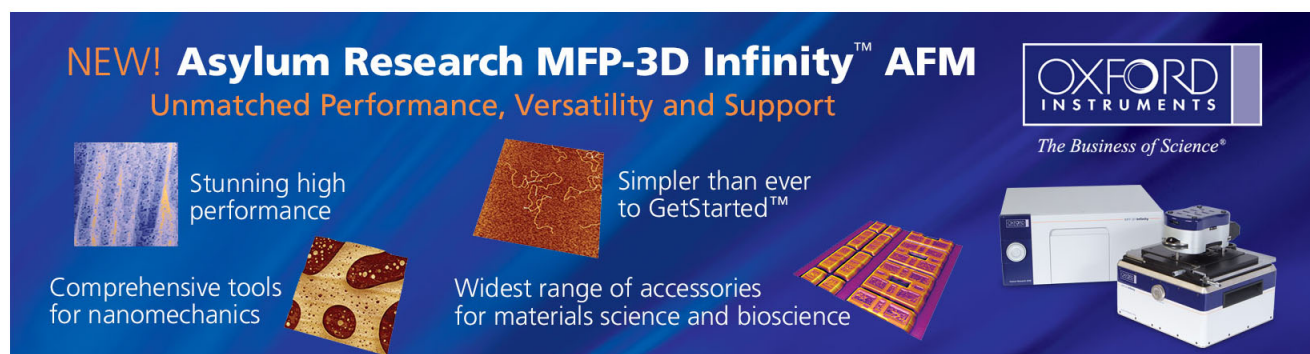
[Site-controlled InAs quantum dots on GaAs patterned using self-organized nano-channel alumina template](#)

*J. Vac. Sci. Technol. B* **23**, 1232 (2005); 10.1116/1.1914824

[Embedding and self-organization of nanoparticles in phospholipid multilayers](#)

*J. Chem. Phys.* **121**, 510 (2004); 10.1063/1.1760077

---



**NEW! Asylum Research MFP-3D Infinity™ AFM**  
Unmatched Performance, Versatility and Support

**OXFORD INSTRUMENTS**  
*The Business of Science®*

Stunning high performance

Simpler than ever to GetStarted™

Comprehensive tools for nanomechanics

Widest range of accessories for materials science and bioscience

*Asylum Research*

# Self-organized titanium oxide nanodot arrays by electrochemical anodization

Po-Lin Chen and Cheng-Tzu Kuo

*Department of Materials Science and Engineering, National Chiao Tung University, Hsinchu, Taiwan*

Tzeng-Guang Tsai, Bo-Wei Wu, Chiung-Chih Hsu, and Fu-Ming Pan<sup>a)</sup>

*National Nano Device Laboratory, Hsinchu, Taiwan*

(Received 3 January 2003; accepted 6 March 2003)

Ordered nanodot arrays of titanium oxides were prepared from TiN/Al films on the silicon substrate by electrochemical anodization of a TiN layer using a nanoporous anodic aluminum oxide film as the template. The microstructure of the nanodot arrays was studied by transmission electron microscopy and scanning electron microscopy, and the chemical composition of nanodots was analyzed by electron energy loss spectroscopy. The as-prepared nanodots are basically composed of amorphous  $\text{TiO}_x$  with a hexagonal arrangement and an average diameter of about 60 nm. Using this approach, it is expected that nanodot arrays of various oxide semiconductors can be achieved.

© 2003 American Institute of Physics. [DOI: 10.1063/1.1571661]

Semiconductor nanodots have attracted great interest because of their unique physical properties and promising applications in optoelectronic and microelectronic devices. They exhibit a wide range of size-dependent properties, and variations in fundamental characteristics ranging from phase transitions to electrical conductivity can be fine tuned by controlling the size of the nanodots. One of the most probable approaches for preparing nanodots for device applications is the self-organized Stranski–Krastranov growth in strained heterostructures.<sup>1</sup> However, the spatial arrangement and size distribution of nanodots are random for most self-organized processes. In order to integrate the nanodots into practical applications, it is necessary to well control the alignment and size of nanodots on the substrate. Many techniques<sup>2–5</sup> have been attempted to control the spatial arrangement and size distribution of nanodots. Ordered arrays of nanodots have been constructed by using nanoporous anodic aluminum oxide (AAO) membranes as an evaporation mask by Masuda *et al.*<sup>5</sup> Nanoporous AAO, which consists of vertical pore channel arrays with a hexagonal packing structure, was obtained by anodic oxidation of aluminum in an acidic electrolyte. The pore diameters are tunable in the range of ten to several hundred nanometers,<sup>6</sup> making AAO an ideal template for fabricating ordered arrays of nanostructured materials.

The majority of previous studies used Al foils to prepare nanoporous AAO films, which must eventually be separated from the Al foil for later applications. This is apparently not suitable for most integrated device applications. Recently, nanoporous AAO has been prepared directly on Al films coated on silicon wafers for integrated microelectronic applications.<sup>7–11</sup> Researches has shown that the microstructure of AAO prepared from Al films on semiconductor<sup>7</sup> or glass<sup>12</sup> substrates are very different from that of AAO obtained directly from Al foils. Beneath each pore bottom, a semispherical nanovoid is formed at the alumina ( $\text{Al}_2\text{O}_3$ ) barrier layer/substrate interface. In the case of anodization of

Al films deposited on a different metal film,<sup>13,14</sup> the anodization process is reported to include two oxidation stages, i.e., anodic oxidations of the Al layer and the underlying metal layer. During the first stage, the nanoporous array is formed, which can then be used as a mask for local anodization of the underlying metal layer, thereby forming a metal–oxide nanostructured array with a similar pattern as the upper AAO nanoporous array. In this letter, we used nanoporous AAO films as the mask for local anodization of titanium nitride (TiN) films to fabricate nanodot arrays of titanium oxide ( $\text{TiO}_2$ ). Using AAO templates as the anodization mask for TiN thin films, we can realize highly ordered arrays of  $\text{TiO}_2$  nanodots with a narrow size distribution. Compared with planar solids,  $\text{TiO}_2$  nanomaterials have been proposed for a wide range of uses including improved solar energy conversion, hydrogen storage, catalysis, and environmental pollution remediation. Using this approach, it is expected that nanodot arrays of many oxide semiconductors, which have an anodization behavior similar to that of  $\text{TiO}_2$ , may be fabricated.

Figure 1 illustrates the anodization steps for the preparation of nanodot arrays of titanium oxides. A sputtered TiN film of about 30 nm in thickness was first deposited on the *p*-Si (100) wafer, followed by deposition of an Al film of 6  $\mu\text{m}$  in thickness by thermal evaporation. The Al film was deposited in a high vacuum chamber ( $<5 \times 10^{-7}$  Torr) using an Al source with a purity of 99.999%. Prior to anodization, the sample was annealed at 500 °C in a vacuum furnace ( $1 \times 10^{-7}$  Torr) for 8 h to recrystallize the Al film, and then electropolished in a mixed solution of  $\text{HClO}_4$  and  $\text{C}_2\text{H}_5\text{OH}$  to obtain a smooth surface. The two-step anodization, which has been reported in detail elsewhere,<sup>15,16</sup> was used to prepare ordered pore channel arrays of AAO. Anodization was first carried out in a 0.3 M oxalic acid solution at 21 °C under a constant polarization voltage of 40 V for 30 min. The resulting nanoporous AAO, about 2  $\mu\text{m}$  in thickness as shown in Fig. 1(a), was removed by wet chemical etching at 60 °C with a mixed solution of  $\text{H}_3\text{PO}_4$  and  $\text{CrO}_3$ , and thereby a relatively ordered indent pattern was produced on the surface of the Al film [Fig. 1(b)]. The second anodization

<sup>a)</sup>Electronic mail: fmpan@ndl.gov.tw

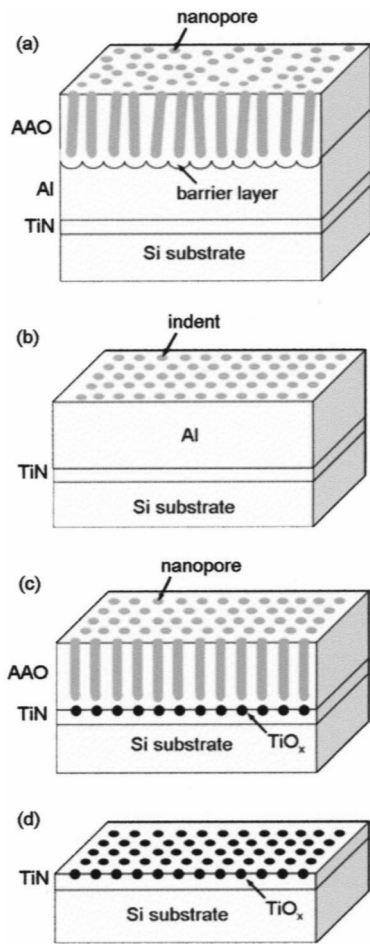


FIG. 1. Schematic diagram of the anodization process for fabrication of the titanium oxide nanodot arrays: (a) First anodic oxidation step, (b) prestructured Al film, (c) second anodization step and TiO<sub>x</sub> nanodot formation, and (d) TiO<sub>x</sub> nanodot arrays. The thickness of the electropolished Al film before anodic oxidation was about 4 μm, and the sputtered TiN layer was 30 nm in thickness.

of the prestructured Al film was then performed for 40 min under the same anodization condition as the first one. After the second anodization step, highly uniform and periodic nanopores were formed [Fig. 1(c)], which were then used as the template for local anodization of the underlying TiN layer. During the anodization of the Al layer, the anodic current density was rather steady at about 8 mA/cm<sup>2</sup> except at the

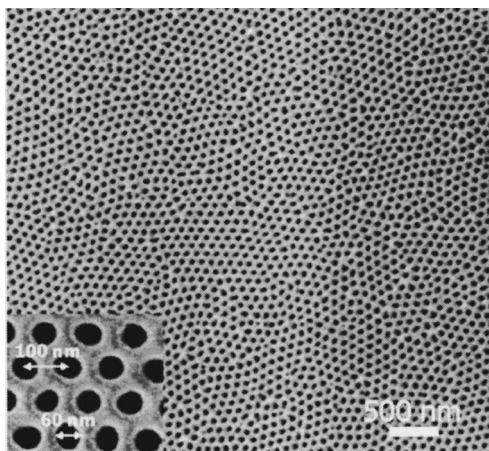


FIG. 2. Top-view SEM image of the nanoporous AAO film after pore widening in a H<sub>3</sub>PO<sub>4</sub> solution. The inset shows a close-up view of the hexagonal arrangement of the nanopores.

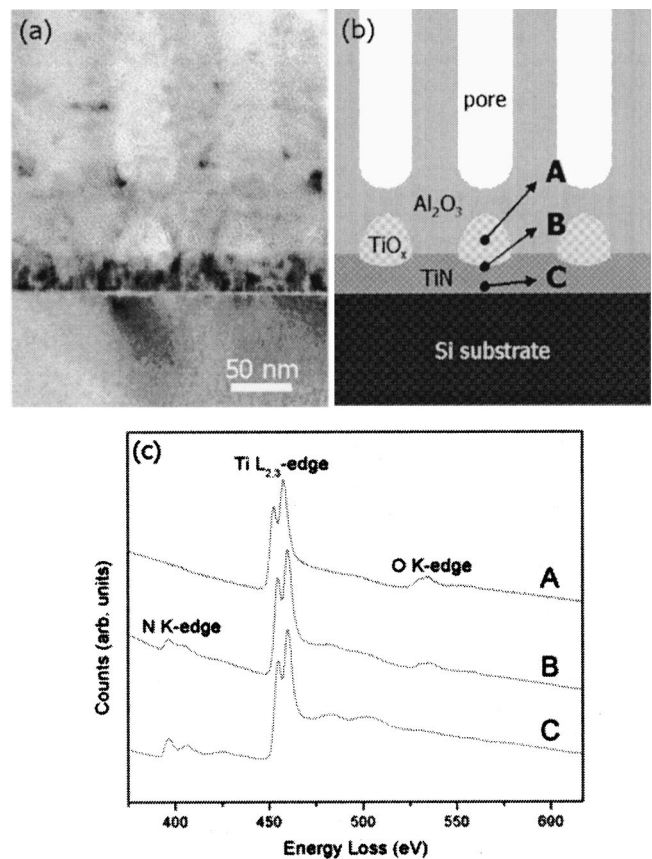


FIG. 3. (a) Cross-sectional TEM image of the bottom of AAO nanopore channels after the completion of the anodization, (b) diagrammatic illustration of the TEM image in (a), and (c) EELS spectra showing the Ti L<sub>2,3</sub> edge, N K edge, and O K edge. The spectra correspond to three different positions as shown in (b): (A) At the center, (B) at the bottom, and (C) at the underside of the dome.

initial stage. The anodic current density dropped abruptly to a value less than 0.1 mA/cm<sup>2</sup> as the oxidation of the Al layer to AAO was completed. When the AAO anodization was in process, the underlying TiN layer was oxidized by anodization as well. The anodic oxidation of TiN layer was confined in the AAO pore area and, consequently, led to the formation of nanodot structures with a pattern in accordance with the upper nanoporous AAO layer.

Figure 2 shows the top-view scanning electron microscopy (SEM) image of the nanoporous AAO film after pore widening in a 5% H<sub>3</sub>PO<sub>4</sub> solution at 30 °C for 30 min. The self-organized nanopores with a uniform size distribution have a pore diameter about 60 nm and an interpore distance about 100 nm. The AAO nanopores do not show a long-range ordering, but within a pore array domain, ordered nanopore with a hexagonal arrangement is clearly observed. Figure 3(a) shows a cross-sectional transmission electron microscopy [(TEM) JEOL JEM-2010F] image of the bottom of nanopores. Figure 3(b) presents a diagrammatic illustration of the TEM image. The TEM image, in Fig. 3(a), clearly shows that there is an isolated dome structure embedded at the interface between the AAO and TiN layer. In order to identify the chemical composition of the dome structure, electron energy loss spectroscopy [(EELS) Gatan GIF 2000] analysis was performed. The detected electrons have undergone core losses within the energy range between 310 and 617 eV, within which the characteristic edges of titanium

( $L_{2,3}$  edge), nitrogen ( $K$  edge), and oxygen ( $K$  edge) were measured.

Figure 3(c) shows the EELS spectra taken at three different positions of the dome structure as indicated in Fig. 3(c). Spectrum A, in Fig. 3(c), was taken at the dome center, which indicates that the dome structure basically consists of titanium and oxygen. However, the fine structure of the oxygen  $K$ -edge peak is not comparable to  $\text{TiO}_2$  from literatures,<sup>17</sup> suggesting that the dome is likely composed of nonstoichiometric  $\text{TiO}_x$ . Spectrum B, in Fig. 3(c), was taken at the dome bottom, and reveals that there is a  $\text{TiN}_x\text{O}_y$  transition layer formed between the underlying TiN layer and the top  $\text{TiO}_x$  dome. With regard to the underlying TiN layer, little oxygen  $K$ -edge peak is detected in the EELS spectrum [spectrum C of Fig. 3(c)] indicating that anodization of the underlying TiN layer was not complete. The EELS study clearly shows that the dome structure was derived from the anodization reaction of the underlying TiN layer. While the anodization process proceeds, an oxygen concentration gradient develops, which correlates closely with the diffusion rate of oxygen containing ions ( $\text{O}^{2-}$  and/or  $\text{OH}^-$ ) from the electrolyte. Thus, anodization of TiN is most efficient in the upper portion of the underlying TiN layer. The  $\text{TiO}_x$  bulge resulting from oxidation of the TiN layer is accompanied by a volume expansion. The molar volume increase is about 60% as TiN is oxidized to  $\text{TiO}_2$ .<sup>18</sup>

The anodization behavior of the TiN/Al film stack on the silicon wafer is regarded to involve two stages and is different from the case of the Al film directly deposited on semiconductor substrates. In the earlier stage, the upper Al layer is anodized to  $\text{Al}_2\text{O}_3$ , accompanied by the simultaneous outward migration of  $\text{Al}^{3+}$  and inward diffusion of  $\text{O}^{2-}/\text{OH}^-$  ions driven by the applied electric field, leading to the vertical pore channel growth.<sup>19</sup> The  $\text{Al}_2\text{O}_3$  dissolution at the  $\text{Al}_2\text{O}_3$ /electrolyte interface is in equilibrium with the  $\text{Al}_2\text{O}_3$  growth at the Al/ $\text{Al}_2\text{O}_3$  interface. As the oxide barrier layer at the pore bottom approaches the area adjacent to the TiN/Al interface, anodization of the underlying TiN can be initiated. The anodic reaction results in the formation of the  $\text{TiO}_x$  bulges. Finally, the anodic current drops abruptly (less than  $0.1 \text{ mA/cm}^2$ ) and the electrochemical reactions terminate due to the complete conversion of remaining Al to  $\text{Al}_2\text{O}_3$ . At the end of the anodic oxidation, the  $\text{Al}_2\text{O}_3$  barrier layer at pore bottom mantles the  $\text{TiO}_x$  dome.

The side-view SEM image of the  $\text{TiO}_x$  nanodot arrays after removing the nanoporous AAO is shown in Fig. 4. The arrangement and shape of the nanodots are in accordance with the nanopores of the AAO template as shown in Fig. 2. This suggests that local anodization of TiN takes place only inside the nanopores. The ordered hexagonal arrangement of the nanodot arrays may be disrupted by domain boundaries. The nanodots of a very high density have an average diameter about 60 nm, which is determined by the pore size of the AAO template. The average height of the nanodots is about 45 nm. The size of the locally anodized nanodots can be varied over a wide range because the diameter of the self-ordered nanopores is dependent upon anodization parameters, such as polarization voltage, bath temperature, electrolyte species, and electrolyte concentration.

In summary, ordered nanodot arrays of titanium oxides

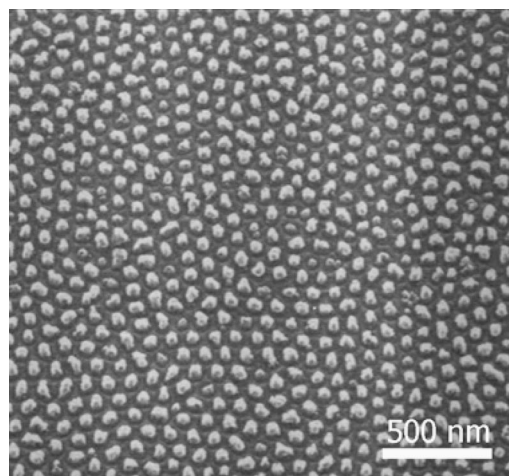


FIG. 4. Side-view SEM image of titanium oxide nanodot arrays after removing the nanoporous AAO template.

were prepared from TiN/Al films on silicon wafers by electrochemical anodization. The hexagonal pore arrays of the AAO templates can faithfully duplicate an ordered pattern for the titanium oxide nanodots. The average size of the nanodots is about 60 nm, which is very close to the diameter of the AAO nanopores, and adjustable depending on anodization conditions. TEM, SEM, and EELS were utilized to determine the microstructure and chemical composition of the nanodots. The as-prepared nanodots are basically amorphous and composed of nonstoichiometric  $\text{TiO}_x$ .

This work was supported partly by the National Science Council (NSC), Taiwan, under Contract Nos. NSC-91-2215-E317-001, NSC-91-2722-2317-200, and NSC-91-2216-E009-028. Technical support from National Nano Device Laboratories is gratefully acknowledged.

- <sup>1</sup>D. J. Eaglesham and M. Cerullo, Phys. Rev. Lett. **64**, 1943 (1990).
- <sup>2</sup>G. Jin, J. L. Liu, S. G. Thomas, Y. H. Luo, K. L. Wang, and Bich-Yen Nguyen, Appl. Phys. Lett. **75**, 2752 (1999).
- <sup>3</sup>T. Kitajima, B. Liu, and S. R. Leone, Appl. Phys. Lett. **80**, 497 (2002).
- <sup>4</sup>X. Mei, D. Kim, H. E. Ruda, and Q. X. Guo, Appl. Phys. Lett. **81**, 361 (2002).
- <sup>5</sup>H. Masuda, K. Yasui, and K. Nishio, Adv. Mater. **12**, 1031 (2000).
- <sup>6</sup>A. P. Li, F. Müller, A. Birner, K. Nielsch, and U. Gösele, Appl. Phys. Lett. **84**, 6023 (1998).
- <sup>7</sup>D. Crouse, Y.-H. Lo, A. E. Miller, and M. Crouse, Appl. Phys. Lett. **76**, 49 (2000).
- <sup>8</sup>S. Shingubara, O. Okino, Y. Murakami, H. Sakaue, and T. Takahagi, J. Vac. Sci. Technol. B **19**, 1901 (2001).
- <sup>9</sup>T. Iwasaki, T. Motoi, and T. Den, Appl. Phys. Lett. **75**, 2044 (1999).
- <sup>10</sup>S.-H. Jeong, H.-Y. Hwang, K.-H. Lee, and Y. Jeong, Appl. Phys. Lett. **78**, 2052 (2001).
- <sup>11</sup>W. Hu, D. Gong, Z. Chen, L. Yuan, K. Saito, C. A. Grimes, and P. Kichambare, Appl. Phys. Lett. **79**, 3083 (2001).
- <sup>12</sup>S. Z. Chu, K. Wada, S. Inoue, and S. Todoroki, J. Electrochem. Soc. **149**, B321 (2002).
- <sup>13</sup>A. Mozalev, A. Surganov, and S. Magaino, Electrochim. Acta **44**, 3891 (1999).
- <sup>14</sup>A. I. Vorobyova, V. A. Sokol, and E. A. Outkina, Appl. Phys. A: Mater. Sci. Process. **67**, 487 (1998).
- <sup>15</sup>H. Masuda and K. Fukuda, Science **268**, 1466 (1995).
- <sup>16</sup>H. Masuda and M. Satoh, Jpn. J. Appl. Phys., Part 2 **35**, L126 (1996).
- <sup>17</sup>H. O. Moltaji, J. P. Buban, J. A. Zaborac, and N. D. Browning, Micron **31**, 381 (2000).
- <sup>18</sup>S. Gwo, C.-L. Yeh, P.-F. Chen, Y.-C. Chou, T. T. Chen, T.-S. Chao, S.-F. Hu, and T.-Y. Huang, Appl. Phys. Lett. **74**, 1090 (1999).
- <sup>19</sup>O. Jessensky, F. Müller, and U. Gösele, Appl. Phys. Lett. **72**, 1173 (1998).